Transfer of Kv3.1 Voltage Sensor Features to the Isolated Ci-VSP Voltage-Sensing Domain

Yukiko Mishina, Hiroki Mutoh, and Thomas Knöpfel*
RIKEN Brain Science Institute, Saitama, Japan

ABSTRACT Membrane proteins that respond to changes in transmembrane voltage are critical in regulating the function of living cells. The voltage-sensing domains (VSDs) of voltage-gated ion channels are extensively studied to elucidate voltage-sensing mechanisms, and yet many aspects of their structure-function relationship remain elusive. Here, we transplanted homologous amino acid motifs from the tetrameric voltage-activated potassium channel Kv3.1 to the monomeric VSD of *Ciona intestinalis* voltage-sensitive phosphatase (Ci-VSP) to explore which portions of Kv3.1 subunits depend on the tetrameric structure of Kv channels and which properties of Kv3.1 can be transferred to the monomeric Ci-VSP scaffold. By attaching fluorescent proteins to these chimeric VSDs, we obtained an optical readout to establish membrane trafficking and kinetics of voltage-dependent structural rearrangements. We found that motifs extending from 10 to roughly 100 amino acids can be readily transplanted from Kv3.1 into Ci-VSP to form engineered VSDs that efficiently incorporate into the plasma membrane and sense voltage. Some of the functional features of these engineered VSDs are reminiscent of Kv3.1 channels, indicating that these properties do not require interactions between Kv subunits or between the voltage sensing and the pore domains of Kv channels.

INTRODUCTION

Specialized proteins that detect electrical potentials across lipid membranes play a central role in fast signaling in brain and muscle and in the regulation of general cellular homeostatic systems. These proteins include voltage-gated ion channels that have voltage-sensing domains (VSDs), formed by four transmembrane segments (S1–S4), and an ion-conducting pore domain. In these channels, voltage-dependent conformational states of the VSD are coupled to the open probability of the ion-conducting pore. Recently, proton-selective channels and voltage-sensitive enzymes with VSDs that are homologous to that of ion channels have been discovered (1–4). The most prominent model within this group of membrane proteins that exist without the pore domain is *Ciona intestinalis* voltage-sensitive phosphatase (Ci-VSP) (1,5–10). Instead of operating an ion pore, the VSD of Ci-VSP is coupled to a cytoplasmic phosphatase that is activated upon depolarization (11,12).

Studies using chimeras of various ion channels have uncovered the functional and structural relevance of specific regions and segments of these channels, including the VSD (13–22). One outstanding example for this approach is the crystallized chimera of Kv1.2 and Kv2.1, which provided the first static view of the structure of a voltage-gated potassium channel in a membrane-like environment (19). Chimeric ion channels with the S1–S4 segments swapped between diverse channel families supported the concept that VSDs are functionally independent modules (14,20). Smaller motifs involving only S4 also appear to be portable modules that are interchangeable between various voltage-gated channels (13,21,22). Functional chimeric ion channels have also been created using segments of Ci-VSP (15,23) demonstrating that the general mechanisms of voltage sensing are similar between voltage-gated ion channels and Ci-VSP. However, segments larger than the paddle region could not be successfully inserted, indicating that there are only a narrow range of Ci-VSP segments that can be transplanted into potassium channel subunits to form voltage-gated chimeric channels (15,23).

Despite having a similar voltage-sensing mechanism, the various VSD-containing proteins exhibit distinctive voltage-dependent kinetic properties. In particular, Kv3.1 channels have very fast activation and deactivation kinetics and they are activated at more depolarized membrane potentials than many other potassium channels (24–26). Consistent with this specialization, Kv3.1 channels are enriched in neurons that fire at high frequencies where they facilitate the repolarization of rapid, narrow neuronal action potentials (27–31). This feature requires very fast (<1 ms) voltage-dependent conformational transitions (i.e., voltage sensor movements). The VSD of Ci-VSP, in contrast, is most sensitive at membrane voltages far above 0 mV and exhibits only modestly fast response kinetics (10,27).

Because Kv channels require subunit tetramerization and formation of a pore to be functional, it is possible that some of their functional properties are the result of an interaction between their subunits. This may explain why Kv subunit regions between S1 to the first half of S3 could not be substituted by homologous segments of Ci-VSP (15,23). To explore this issue, we investigated the portability of VSD segments in the reverse direction and transplanted homologous amino acid motifs from the Kv3.1 subunit to the monomeric VSD of Ci-VSP. We found that motifs extending from 10 to roughly 100 amino acids can be readily

Submitted May 24, 2012, and accepted for publication July 23, 2012.

*Correspondence: tknopfel@brain.riken.jp

Editor: Eduardo Perozo.

0006-3495/12/08/0669/8 $2.00

http://dx.doi.org/10.1016/j.bpj.2012.07.031

transplanted from Kv3.1 into Ci-VSP to form functional chimeric proteins that incorporate into the plasma membrane and sense voltage. Some of the functional features of these engineered, self-sustained voltage-sensing domains are reminiscent of Kv3.1 channels, indicating that these properties are independent of subunit stoichiometry and do not require the presence of the pore domain.

MATERIALS AND METHODS

Molecular biology and expression

Chimeric constructs were generated using sequential polymerase chain reactions with mKv3.1 and VSFP2.3 (for Ci-VSP-based constructs) as templates in pcDNA3.1(−) backbone (27). Ci-VSP contained the R217Q mutation. DNA sequences for all constructs were confirmed by DNA sequencing analysis. Sequences were aligned using ClustalW2 (EMBL-EBI). PC12 cells were cultured in Dulbecco's modified Eagle's medium supplemented with 10% horse serum, 5% fetal bovine serum, and 1% penicillin and streptomycin (GIBCO) at 37°C. Cells were grown on coverslips and transfected 24 h after plating using Lipofectamine 2000 reagent (Invitrogen) and washed daily. Experiments were performed 2–3 days after transfection.

Optical imaging and electrophysiology

PC12 cell images were obtained with a confocal laser scanning microscope (C1si/FN1, Nikon). For electrophysiology, cells on coverslips were mounted on an inverted microscope equipped with epifluorescence optics (Eclipse TE2000-U, Nikon). Voltage-dependent fluorescence recordings from PC12 cells were performed by combining voltage clamp (under the whole-cell configuration of the patch-clamp technique) with dual-emission microfluorometry. Data acquisition was performed using pCLAMP 8.0/10.1 software (Axon Instruments). PC12 cells were continuously perfused (1.5–2 ml/min) with a bathing solution containing (in mM) 150 NaCl, 4 KCl, 2 $CaCl_2$, 1 $MgCl_2$, 5 Glucose, 5 HEPES (pH 7.4). Patch electrodes were pulled from standard walled, borosilicate glass capillaries (Hilgenberg) using a two-stage puller (PP-830, Narishige), and had resistances of 3–5 mOhm when filled with intracellular solution containing (in mM) 130 CsCl, 1 $MgCl_2$, 20 HEPES, 5 EGTA, 3 MgATP (pH 7.2). All data were low pass filtered with a cutoff frequency of 5 kHz and digitized at 5 kHz using a Digidata 1200/1322 analog-to-digital converter (Axon Instruments). Fluorescence was induced by light from a computer-controlled monochromator (Polychrome IV, T.I.L.L. Photonics) through a 50× oil immersion objective. Excitation light (440 nm) was reflected and first passed through a 458-nm dichroic mirror (FF458-Di01, Semrock). Emitted light was then split by a 506-nm dichroic mirror (FF506-Di03, Semrock) onto two photodiodes (T.I.L.L. Photonics) behind Cerulean- and Citrine-specific filters (BP 482 ± 35 nm: FF01-482/35-25 and LP 514 nm: LP02-514RU-25, Semrock). Photodiode signals were digitized along with the electrophysiological signals using Axon hard- and software.

We used the following protocol to test VSD function. From a holding voltage of −60 mV, cells were held for 500 ms at voltages between −100 and 60 mV or between −120 and 100 mV in 20 mV steps to elicit fluorescence signals from cyan fluorescent protein (CFP) and yellow fluorescent protein (YFP). Background data were obtained from a region on the coverslips devoid of fluorescent proteins. Photobleaching was corrected by division of a double exponential fit of the fluorescence trace at the holding potential. The ratiometric fluorescent signals were obtained by dividing the signals from the two fluorescent proteins. Time constants were obtained by fitting single or double exponential decay functions to the activation and deactivation curves for each plot. The dynamic range (ΔR/R) was calculated as the absolute change in the magnitude of fluorescence at −100 and 60 mV of the ratiometric fluorescence signals from the holding potential of −60 mV. The $V_{1/2}$ was obtained by plotting the ΔR/R against voltage in 20 mV steps, and each plot was fitted with a Boltzmann function $1/(1 + \exp((V_{1/2}–V)/k))$ where $V_{1/2}$ is the half-activating potential and k is the slope factor. Data were analyzed using Clampfit 10.2 software (Axon), MATLAB (The MathWorks, Natick, MA), and Origin 8.1. Data are expressed as mean ±SE, with n specifying the number of independent experiments. For each cell and voltage protocol, 6–8 traces were averaged.

The initial screening of constructs where we determined the initial dynamic range (%ΔR/R; see Fig. 2, Table S3) was performed at ambient temperature (23 ± 2°C), whereas the detailed kinetic characterizations were based on experiments conducted at 31 ± 1°C in view of the possible application of the chimeric voltage-sensing domains as optical probes for mammalian membrane potential. Comparison of detailed kinetic characterizations performed at ambient temperature (23 ± 2°C) revealed slower kinetics and modest differences in voltage dependency (~10 mV) but a similar dynamic range (Table S2).

RESULTS

We constructed chimeric voltage sensors in which portions of Ci-VSP VSD were replaced with homologous segments of Kv3.1. Because these chimeric proteins do not contain an ion channel-forming pore, measurement of ionic currents cannot be used as an indicator of voltage sensing. We therefore used the design of a fluorescent protein-based voltage indicator in which a pair of fluorescent proteins is attached to the C-terminus of a VSD to establish trafficking to the plasma membrane and responsiveness to changes in membrane potential (Fig. 1 *A*) (28). As a reference and control, we used the native Ci-VSP VSD (except for the R217Q mutation, see below) attached to CFP and YFP, a construct named VSFP2.3 (27). To identify homologous segments of Kv3.1 and Ci-VSP, we aligned the sequences as shown in Fig. 1 *B*.

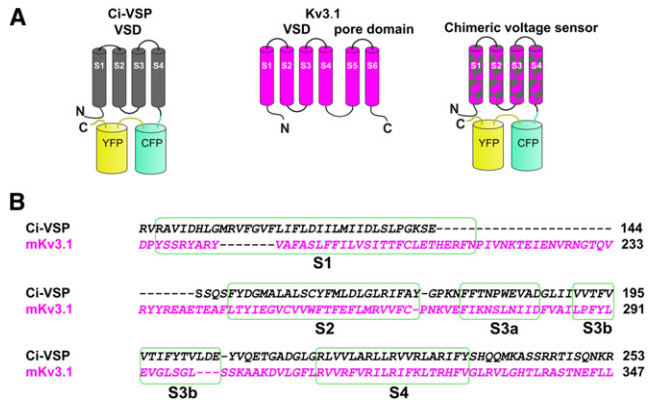

FIGURE 1 Designing chimeric constructs between Ci-VSP and Kv3.1 in the VSD. (*A*) Schematic depiction of (from *left* to *right*) the Ci-VSP VSD fused with a pair of fluorescent proteins (CFP and YFP), the topology of a Kv3.1 subunit and a chimeric construct involving components of the former two structures. The pair of fluorescent proteins enables visualization of membrane targeting and monitoring of voltage-dependent movements of the VSD. (*B*) Sequence alignment of the S1 to S4 transmembrane segments of Ci-VSP and mKv3.1. The alignment was shifted for two constructs (C37 and C38) in the S1 region (Table S1).

Functional chimeric voltage sensors with a broad range of transplanted segments

We generated 40 chimeras by transferring various portions of varying lengths from Kv3.1 into Ci-VSP (Fig. 2), and evaluated the efficiency of trafficking to the plasma membrane by confocal fluorescence imaging (Fig. 3). Surprisingly, over half of these chimeras localized to the plasma membrane. Only those chimeras in which the entire N-terminus or internal portion of S1 was exchanged consistently demonstrated poor membrane targeting (Fig. 3 *B*), whereas ~90% of the remaining chimeras localized to the membrane. We introduced a single point mutation (R217Q), which shifts the voltage dependency to a range closer to the typical resting potential of mammalian cells. This point mutation, which shifts the $V_{1/2}$ 130 mV to the left (6,28), was retained in all

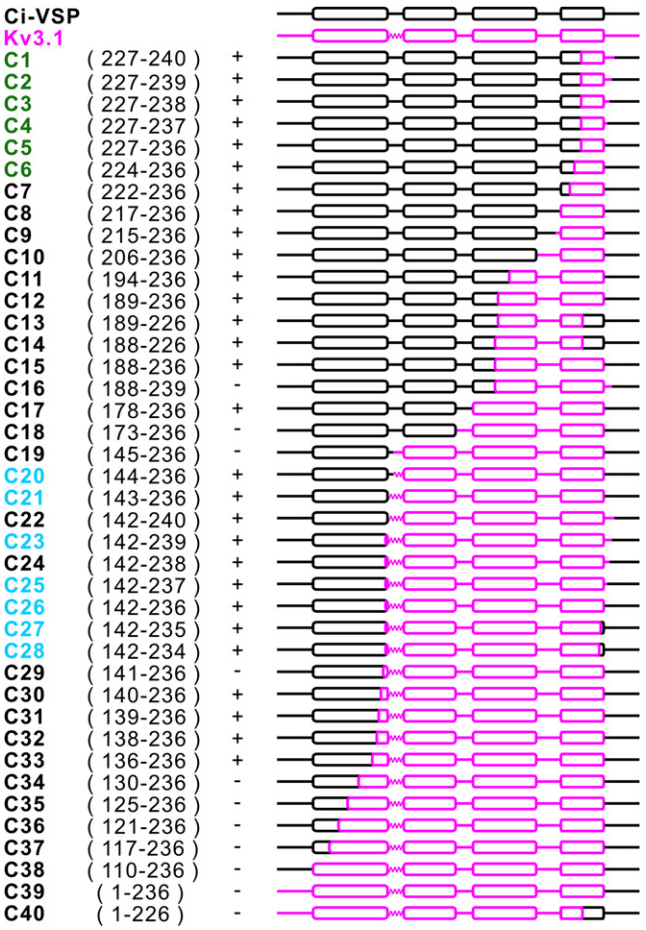

FIGURE 2 Chimeras made by transferring segments of Kv3.1 to Ci-VSP. Amino acids in Ci-VSP that were substituted by homologous residues in Kv3.1 are indicated after the construct name in the first column. The membrane-targeted constructs are denoted by +, whereas absence of membrane targeting is indicated by −. All constructs that showed targeting also showed voltage-dependent modulation of FRET efficacy. Colored names indicate chimeras that exhibited ΔR/R signals >5%. The % ΔR/R values of each of the chimeras (n = 6–13), calculated from test potentials of −100 and 60 mV from a holding potential of −70 mV, are provided in Table S1.

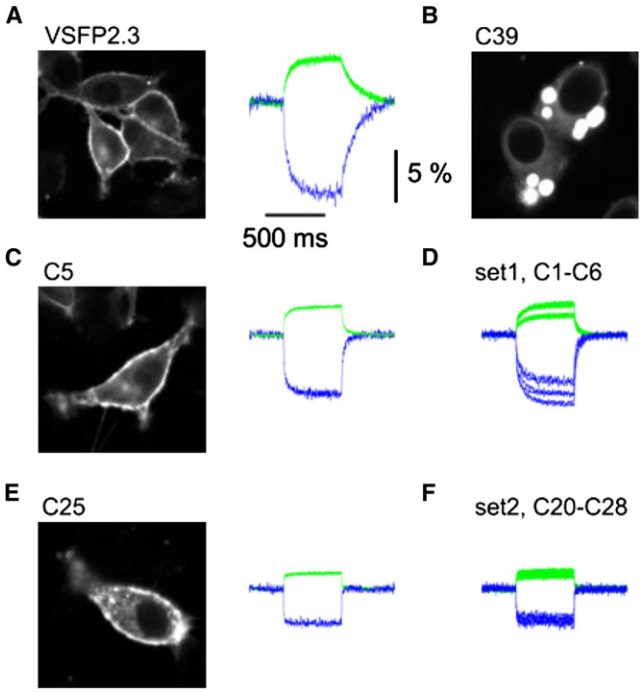

FIGURE 3 Plasma membrane localization and voltage-dependent FRET efficacy modulation. (*A*) Membrane targeting and FRET signals of the control construct VSFP2.3 expressed in PC12 cells. Fluorescent signals of donor (CYP, *blue trace*) and acceptor (YFP, *green trace*) upon depolarization to 60 mV from a holding voltage of −70 mV. n = 9. (*B*) Fluorescence image of a chimera (C39) that failed to traffic to the membrane of PC12 cells. (*C*) Fluorescence image of a construct (C5, n = 6) that localized to the plasma membrane (*left*), and its voltage-dependent FRET modulation (*right*). (*D*) An overlay of ΔR/R signals from all six chimeras containing a substituted segment of S4 from Kv3.1 (C1–C6; n = 6–8) that elicited a large change in FRET efficacy (>5% ΔR/R, highlighted in *green* in Fig. 2). (*E*) Corresponding data from a construct (C25, n = 13) in which a large fragment of the VSD (from the S1-S2 linker to the end of the S4) had been exchanged. (*F*) Overlaid ΔR/R signals from seven other chimeras containing similar substitutions (highlighted in *blue* in Fig. 2; n = 6–13) with functional characteristics similar to C25. Scaling is the same for all fluorescence traces and as indicated by the calibration bar in *A*.

our chimeras except those in which residue R217 was replaced by the corresponding amino acid of Kv3.1. We tested the membrane-targeted chimeras for voltage-dependent modulations of fluorescence resonance energy transfer (FRET) efficiency and found that they all showed a decrease in cyan emission and increase in yellow emission while stepping the membrane voltage from a holding potential of −70 to 60 mV, similar to the reference construct VSFP2.3 (Fig. 3). These FRET signals indicated chimera functionality and confirmed that the VSD of Ci-VSP is receptive to large portions of the protein being substituted by corresponding segments of the Kv3.1 potassium channel (Fig. 2). This finding was surprising in view of the fact that the introduction of replacements in Kv2.1 using portions of Ci-VSP larger than the paddle (S3b-S4) consistently yielded nonfunctional chimeric proteins (15). We were also able to extend the exchanged region into the C-terminal portion of S4, which

resulted in a loss of function when Ci-VSP was inserted into Kv2.1 (15). In general, the VSD of Ci-VSP proved very accommodating and we found that broad size variations can be tolerated, ranging from a small segment of S4 to as much as three-quarters of the entire VSD.

For a more detailed analysis, we focused on the chimeras that displayed large changes in FRET efficacy (>5% ΔR/R), calculated as the difference between the maximum and minimum of the fluorescence-voltage relationship, in response to voltage changes from a holding potential of −70 to −100 and 60 mV. We interpreted a robust modulation of FRET efficacy as an indicator of a well-operating voltage-sensing mechanism. Two sets of very diverse chimeras (whose names are highlighted in *green* and *blue* in Fig. 2) satisfied this criterion. One set, containing six variants (C1–C6), contained substitutions in a small fragment of the C-terminal end of S4. The other set, containing seven chimeras (C20, C21, C23, and C25–C28), featured an exchange of a large fragment stretching from the S1-S2 linker region to the end of S4. Within each set, the variants only differed from one another by increments of one amino acid, and showed only small differences in their voltage-dependent fluorescent signals (Fig. 3, *D* and *F*).

Functional properties of chimeras with C-terminal end of S4 transplanted

For chimeras C1–C6, the length of the Kv3.1 motif ranged from 10 (between V227 and S236 of Ci-VSP) to 14 (between V227 and M240) amino acids. In all cases but one, the ΔR/R for these chimeras was larger than that of Ci-VSP, ranging from 14.8% to 19.7% across the full range tested (−140 to 120 mV) (Table 1). They showed a general tendency to become more voltage-sensitive with each additional Kv3.1 amino acid insertion, up to a certain maximal length.

The optical response of VSFP2.3 (Fig. 4 *A*, *upper*) to a depolarizing step in membrane voltage to 20 mV from holding potential consists of both a fast and a slow component, with time constants of around 3 and 70 ms, respectively (Table 1). The two voltage-dependent time constants upon depolarization reflect the transition among three major conformational states of the VSD that have been termed, in analogy to corresponding states in Kv channels, deactivated, activated, and relaxed (29,30). Chimera C5 (Fig. 4 *A*, *lower*) showed similar two-component response characteristics, with fast (2.1 ± 0.5 ms) and slow (36.8 ± 2.7 ms) time constants at 20 mV (Fig. 4 *B*, *left*). In contrast to the Ci-VSP VSD, the fast response component in C5 was more dominant and consistently faster (Fig. 4 *C*), contributing to 60% of the total response as compared to 26% in VSFP2.3 (Table 1). More striking are the differences in deactivation (Fig. 4 *B*, *right*) following a hyperpolarizing voltage step, which fits well with a single time constant and is much faster for C5 (13.4 ± 1.5 ms) than for VSFP2.3 (91.6 ± 4.2 ms).

All six chimeras in this set, in which the C-terminus of S4 was exchanged, efficiently trafficked to the membrane, showed changes of FRET efficacy >5% ΔR/R, and exhibited properties quite similar to C5 at 20 mV (Fig. 3 *D*). Although the time constants, the proportion of the two activation components and the dynamic range were all very similar, detailed analysis showed that voltage dependency varied in this set of chimeras (Table 1). The activation voltage dependency of the fast component of C5, which had the smallest amino acid substitution, was only slightly right-shifted compared to VSFP2.3 ($V_{1/2}$ of −18 and −28 mV, respectively), whereas the slow component was shifted more dramatically to more positive membrane potentials (>20 mV vs. −48 mV in VSFP2.3) (Fig. 4 *D*). In comparison, the $V_{1/2}$ of the others in this set ranged from −45 to +11 mV for the fast component, whereas the slow

TABLE 1 Summary of Ci-VSP-Kv3.1 VSD chimeras with ratiometric fluorescence signals >5%

	τ_1 on	τ_2 on	% τ_1	τ_1 off	$V_{1/2}$ fast	$V_{1/2}$ slow	$V_{1/2}$ off	ΔR/R (%)†
VSFP2.3	3.0 ± 0.4	69.2 ± 4.3	26.6	91.6 ± 4.2	−28.3 ± 1.3	−48.6 ± 1.2	−28.2 ± 0.9	15.2 ± 0.2
C1	2.6 ± 0.6	34.9 ± 1.8	62.8	12.8 ± 0.6	11.0 ± 2.1	≥20	≥20	17.9 ± 0.3
C2	2.2 ± 0.4	39.2 ± 1.7	59.7	17.0 ± 0.6	−20.0 ± 2.2	≥20	≥20	19.7 ± 0.6
C3	2.6 ± 0.7	53.0 ± 1.6	52.8	11.1 ± 1.8	−29.2 ± 2.8	≥20	≥20	16.4 ± 0.3
C4	2.3 ± 0.7	45.6 ± 2.5	54.0	15.1 ± 1.3	n/a*	≥20	≥20	16.2 ± 0.2
C5	2.1 ± 0.5	36.8 ± 2.7	60.1	13.4 ± 1.5	−17.9 ± 1.2	≥20	≥20	14.8 ± 0.2
C6	2.2 ± 0.6	54.0 ± 2.7	41.6	18.2 ± 2.1	−45.0 ± 1.7	−4.9 ± 0.8	−16.2 ± 0.4	15.9 ± 0.1
C20	1.9 ± 0.2	n/a	100	1.8 ± 0.3	−26.5 ± 0.5	n/a	−24.8 ± 1.8	5.2 ± 0.4
C21	1.9 ± 0.2	n/a	100	2.0 ± 0.3	−31.9 ± 0.6	n/a	−31.8 ± 0.6	5.6 ± 0.3
C23	2.2 ± 0.1	n/a	100	2.0 ± 0.2	−29.8 ± 0.5	n/a	−29.1 ± 0.5	6.5 ± 0.3
C25	1.8 ± 0.1	n/a	100	1.8 ± 0.2	−27.6 ± 1.8	n/a	−25.6 ± 0.5	6.4 ± 0.3
C26	1.6 ± 0.2	n/a	100	1.9 ± 0.3	−29.3 ± 2.8	n/a	−26.6 ± 0.6	5.8 ± 0.4
C27	1.7 ± 0.2	n/a	100	2.0 ± 0.3	−13.2 ± 0.4	n/a	−11.0 ± 1.2	6.4 ± 0.4
C28	2.2 ± 0.2	n/a	100	2.6 ± 0.2	−15.1 ± 1.5	n/a	−16.7 ± 1.2	5.5 ± 0.3

*$V_{1/2}$ of the fast component of activation of C4 was indeterminable as the fluorescence versus voltage was linear between −140 and 120 mV and could not be fit by the Boltzmann function.

†% ΔR/R values were obtained from the maximal and minimal acceptor/donor florescence ratio responses between −140 and 120 mV (for VSFP2.3, $n = 9$ and for chimeras C1-6; $n = 6–8$) or −100 and 60 mV (for chimeras C20-C28; $n = 6–13$) from a holding potential of −70 mV. Errors, ± SE.

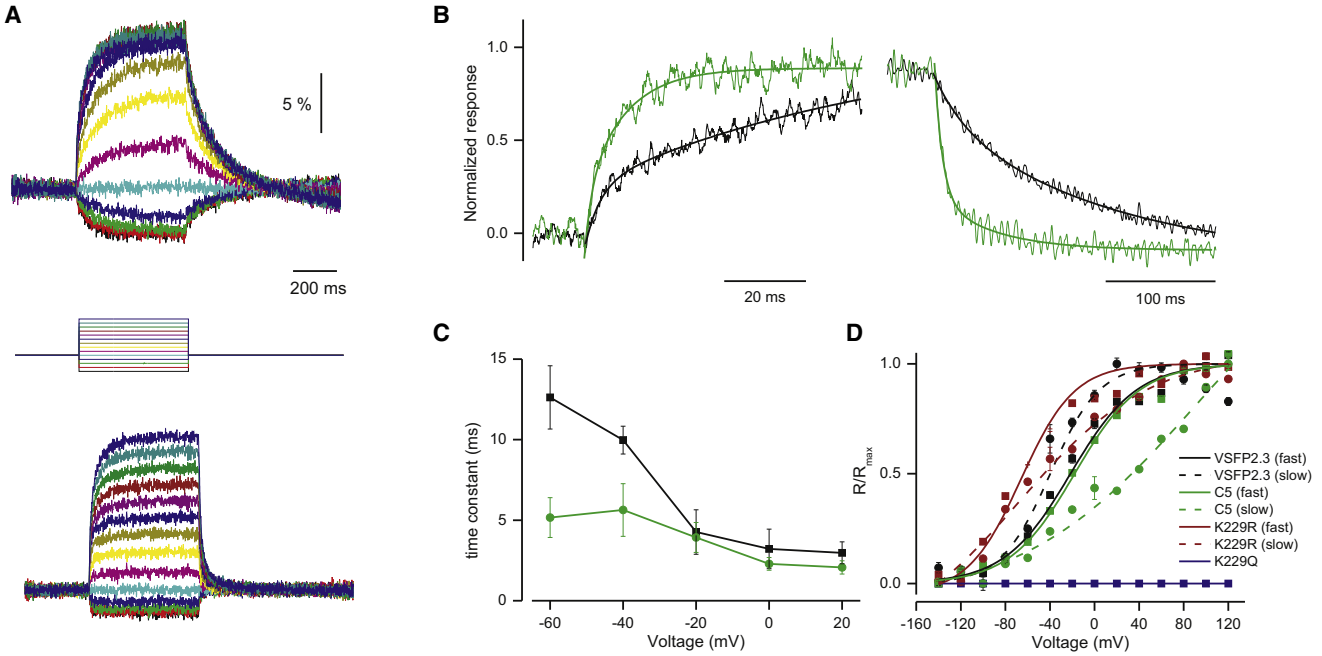

FIGURE 4 Kinetics of voltage dependency of C5, a chimera containing a substitution in S4. (*A*) Comparison of ratiometric fluorescence signals of VSFP2.3 (*upper*) and C5 (*lower*) in response to a family of voltage steps (holding potential −60 mV, 20 mV step increments from –140 to 120 mV). $n = 6$. (*B*) Normalized responses to depolarization (*left*) from −60 to 20 mV and responses to return (*right*) for VSFP2.3 (*black*) and C5 (*green*). The responses were fit with a double exponential decay (*left*) or a single exponential decay (*right*). (*C*) Voltage dependence of time constants for the fast component of activation for VSFP2.3 (*black*) and C5 (*green*). (*D*) Amplitude of normalized FRET efficacy modulation versus membrane voltage for the fast (*solid line*) and slow (*dotted line*) components of VSFP2.3 (*black*), C5 (*green*), and C5-based point mutants (K229R, *maroon*; $n = 6$ and K229Q, *dark blue*; $n = 4$). Error bars, ± SE.

component was >20 mV for all except one (C6, −4.9 mV). In this span, especially in the S4-S5 linker region, the charge and polarity of the amino acids differ drastically between Ci-VSP and Kv3.1, and we found that a single mutation in this region can greatly affect voltage dependency without affecting the general motion (i.e., speed of movement) of the voltage sensor.

Positive charges in the S4 segment

Both Kv3.1 and Ci-VSP have the same number of arginines in the S4 transmembrane segment. Kv3.1 also has a lysine at the C-end of S4 corresponding to an arginine in Ci-VSP (R229) (Fig. 1 *B*). This fifth amino acid interacts with a phenylalanine side chain and the preferences for arginine versus lysine at this position appear predetermined due to functional roles of the proteins (31). To uncover the influence of this lysine, we characterized two mutants based on C5 where we changed the lysine to a glutamine or arginine. We found that a single same-charge point mutation at this position (K229R) (32) dramatically shifted the dependency to the left, whereas neutralization (K229Q) entirely abolished voltage-dependent FRET efficacy modulation despite expression and targeting in the membrane (Fig. 4 *D*). In Kv channels, two consecutive S4 arginines may be deleted without affecting voltage gating (33). Here, we found that C5 mutants in which we had neutralized two nonconsecutive positive charges, corresponding to the first and fifth (R217Q and K229Q) in S4, exhibited no voltage-dependent movement between −100 and 120 mV.

Chimeras with substitutions from the S1-S2 loop region to the end of S4

The second set of chimeras that displayed large (>5% ΔR/R) voltage-dependent FRET efficacy modulation had a large portion of the Kv3.1 sequence transplanted into Ci-VSP. When we replaced the short Ci-VSP S1-S2 linker with the long linker from Kv3.1, the resulting chimeric proteins (C20, C21, C23, C25–C28) successfully targeted to the membrane. However, the deletion of many amino acids to keep the linker shortened to the length of Ci-VSPs led to chimera C19, which did not localize to the plasma membrane. Like the other members of this set, C25 showed a faster voltage-dependent structural rearrangement relative to Ci-VSP (Fig. 5 *A*). Unlike Ci-VSP or chimeras with S4 substitutions, their response to voltage steps was monoexponential for both activation and deactivation (Fig. 5 *B*).

This set of chimeras displayed ~50% of the maximal FRET efficacy modulation observed for the S4-substituted set, ranging from 5.2% to 6.5% ΔR/R (Table 1). In general, most of the chimeras in this set showed a half-maximal activation that was very similar (differing by only ± 2.1 mV) to that of VSFP2.3. For all, the $V_{1/2}$ of deactivation was equal

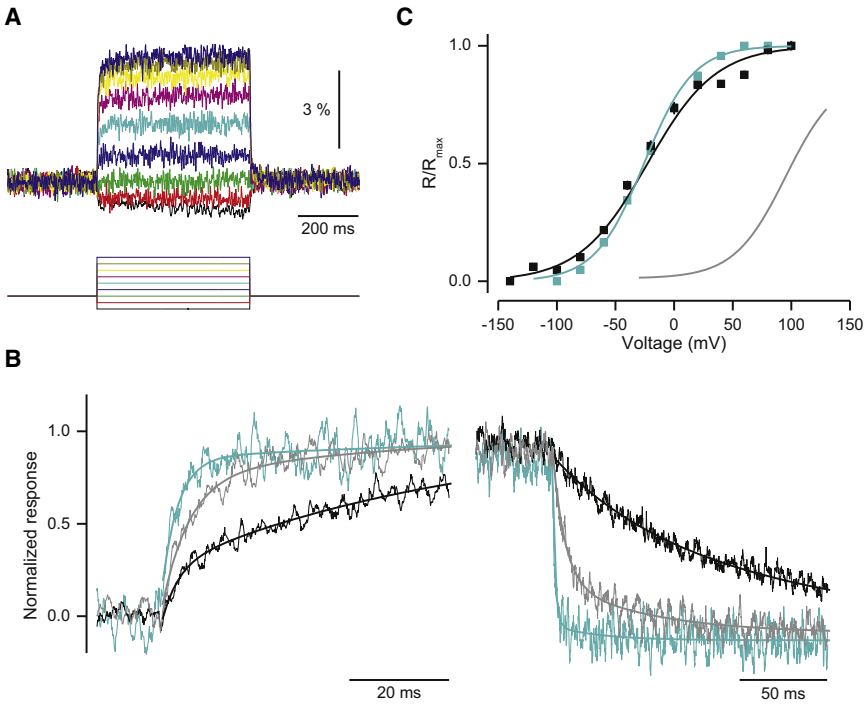

FIGURE 5 Kinetics of C25, a chimera containing a large substitution (S1–S4) from Kv3.1. (*A*) Ratiometric fluorescence signals of C25 in response to a family of voltage steps (holding potential −60 mV, 20 mV step increments from –100 to 60 mV). $n = 13$. (*B*) Normalized responses to depolarization from −60 to 20 mV (*left*) and repolarization (*right*) for C25 (*blue*), VSFP2.3 (*black*), and C5 (*gray*). The responses were fit with a single exponential decay for C25. (*C*) Comparison of fluorescence-voltage relationship of C25 (*blue*) and VSFP2.3 (*black*) as a function of membrane potential. The gray curve represents the voltage dependency of the native (R217) Ci-VSP VSD. Error bars, ± SE.

to that of activation. The F-V curve of C25 is steeper than the other chimeras (Fig. 5 *C*), a feature suggesting increased recruitment of gating charges. Similar to the S4-exchanged set of chimeras, we found two S1-S2 linker chimeras (C27 and C28) where single amino acid mutations shifted the voltage dependency ~14 mV to the right without greatly affecting other properties. Notably, the Kv3.1 replacement also removed the R217Q mutation that had been introduced in Ci-VSP and the S4-exchanged chimeras mentioned previously, indicating that the native Kv3.1 VSD sequence confers a leftward shift in voltage-dependency relative to the native Ci-VSP VSD.

DISCUSSION

Ion channels and several other voltage-sensitive proteins have an S1–S4 transmembrane VSD that plays a fundamental role in the voltage-sensing mechanism. Chimeric tetramer-subunit forming channels have been used to investigate the highly conserved residue pattern of S4 and the slightly extended paddle regions of VSDs (15,23,33), providing evidence that this region does not coevolve with amino acids elsewhere on the channel. Here, we have expanded these chimeric VSD studies beyond the paddle regions and showed, to our knowledge for the first time, that ion channel segments can be functionally transplanted into the monomeric voltage sensor scaffold of Ci-VSP.

We discovered that diverse fragment substitutions with varying lengths extending from S1 to S4 could give rise to proteins that are efficiently targeted to the plasma membrane and exhibit intact voltage-dependent structural rearrangements. The less restrictive portability observed in this study as compared to the study of Alabi et al. (15) may be explained by the lack of interaction of a pore domain with the VSD in Ci-VSP. While performing substitutive transfers containing the external portion of S1, we found one construct, C29 that did not target in the membrane. However, extension or reduction of the exchanged segment by only one amino acid resulted again in a well-targeted construct (see C29 vs. C26 and C30). Interestingly, a single point mutation in this specific region of S1 can disrupt ion channel function (18,34). Because the substitution of amino acids that contact or interact with other parts of the protein may disrupt or significantly alter function or even trafficking, our observation aligns with investigations in ion channels that have proposed that certain amino acids have coevolved to secure or maintain anchoring interactions between specific sites on S1 and other parts of the protein (18,34–36).

Another region that may be involved in obligatory interactions between different parts of the protein or other Kv subunits is the N-terminal region of Kv3.1 extending into S1. This region may be necessary for the tetramerization of subunits in the endoplasmic reticulum (ER) before they traffic to the plasma membrane (37,38). When we elongated the Kv3.1 substitution beyond a particular section of S1, we found that the N-terminus and the first half of S1 in Ci-VSP could not be replaced without losing proper protein folding or trafficking. These results suggest that this N-terminal region may be critical in the proper assembly of voltage-sensitive proteins, and that the N-terminus of Ci-VSP is specifically necessary for the functional formation of

Ci-VSP-based chimeras. Therefore, there may be specific amino acids or sequences that evolved in Ci-VSP but not in other heteromeric voltage-dependent proteins that allow Ci-VSP to function in a voltage-dependent manner as a monomer, unaccompanied by a pore region.

One region that can readily be exchanged among voltage-sensitive proteins is S4. In this region, positively charged arginines play an important role in the coupling of the membrane electric field to VSD conformational states as they sense changes in membrane potential (39). The fifth positive charge in S4 of Kv3.1 is a lysine rather than an arginine, and as mutations of arginine residues in the S4 can result in both positive and negative shifts of the activation curves (28,31,40,41) and even loss of voltage dependency (41), we made two mutants K229Q and K229R to determine the effect of neutralization and same-charge point mutations at this position. In chimeras where we mutated the 5th positive residue in the Kv-derived S4 segment to a glutamine (K229Q), we observed no fluorescence signal associated with changes in voltage from −100 to 120 mV. Although we saw no movement of the S4 following this charge neutralization, it is possible that this construct could be activated at extremely high or low voltages (>120 or <140 mV); this could not be tested in our hands, as it is beyond the capacity of the cells being tested. Another study has shown that Ci-VSP variants containing a double charge neutralization mutation at the same position (R229Q) and at the consecutive arginine (R232Q) showed no movement of S4, although the protein was properly targeted to the cell surface (1), and we discovered that just one mutation at position 229 had the same effect. We also found that a charge-conservation mutation at the same location (K229R) resulted in a shift of the F-V curve to the left. This effect was also observed in the activation of sodium channels, namely NaChBac, where the replacement of the 5th and 6th S4 arginines with lysines led to a shift in the midpoint potential to a more depolarized voltage (40). This 5th lysine has been shown to stabilize the voltage sensor in the open conformation due to interactions with residues in the S2 and S3a (31) in alignment with the function of the Kv3.1 channel to be activated at depolarized potentials. The association of this phenomenon with single point mutations in the voltage sensor emphasizes the significance of positive charges in the S4 transmembrane domain.

The attachment of fluorescent probes to proteins enables characterization of the kinetics of voltage-dependent conformational changes in the VSD (42,43). We found two sets of chimeras that exhibited robust voltage-dependent modulation of FRET efficacy, and followed up with detailed kinetic analyses. A FRET reporter revealed that the VSD of Ci-VSP exhibits voltage-dependent conformational rearrangements in which the kinetics can be described with two distinct voltage-dependent time constants. Previous studies have proposed that the initial fast component corresponds to the time course of the sensor, whereas the subsequent slower component associates with the change in conformation from the active state to a relaxed state (29,30). A relaxed state exists for both Kv3.1 (26,44) and Ci-VSP (30), and is reached upon the transition of the VSD into a more stable conformation during long-lasting depolarization. For our control construct VSFP2.3, we observed a slow time constant that appeared to reflect this relaxed state, with a $V_{1/2}$ that does not depend on temperature (Table S2), in agreement with results previously reported for Ci-VSP and the phosphatase-removed Ci-VSP (30,45). However, we found that by transplanting regions of Kv3.1 into Ci-VSP, the fraction of the slow component decreased proportionally as the size of the Kv3.1 segment increased (73% for VSFP2.3, 40–60% for chimeras with only S4 exchanged, and <1% for chimeras with S1–S4 exchanged, Table 1). The exact reason for this decrease in the percentage of slow component is unclear, but it appears that the substitutions may make the relaxed state less favorable. Alternatively, the transition from the activated to the relaxed states may be either very rapid or undetected by the optical readout in the chimeras with substitutions from the S1-S2 loop region to the end of S4.

This decrease in the amplitude of the slow component of the fluorescence signal combined with faster kinetics are highly desirable features in genetically encoded indicators of membrane voltage that allow for a direct visualization of electrical activity in genetically defined populations of cells (46–48). We showed that transplantation of Kv3.1 segments into the Ci-VSP VSD led to chimeras with fast kinetic characteristics resembling that of Kv3.1. We expect that the engineered VSDs described here will facilitate the generation of improved voltage indicators for detecting fast electrical signals in both neurons and muscles.

SUPPORTING MATERIAL

Three tables are available at http://www.biophysj.org/biophysj/supplemental/S0006-3495(12)00807-7.

We thank all members of the Knöpfel laboratory for helpful discussions, and Atmika Paudel for help throughout this project.

This work was funded by grants from RIKEN Brain Science Institute (to T.K.) and the Ministry of Education, Culture, Sport, Science and Technology of Japan (to H.M.).

REFERENCES

1. Murata, Y., H. Iwasaki, …, Y. Okamura. 2005. Phosphoinositide phosphatase activity coupled to an intrinsic voltage sensor. *Nature.* 435: 1239–1243.
2. Sasaki, M., M. Takagi, and Y. Okamura. 2006. A voltage sensor-domain protein is a voltage-gated proton channel. *Science.* 312: 589–592.
3. Ramsey, I. S., M. M. Moran, …, D. E. Clapham. 2006. A voltage-gated proton-selective channel lacking the pore domain. *Nature.* 440:1213–1216.

4. Hossain, M. I., H. Iwasaki, …, Y. Okamura. 2008. Enzyme domain affects the movement of the voltage sensor in ascidian and zebrafish voltage-sensing phosphatases. *J. Biol. Chem.* 283:18248–18259.
5. Sakata, S., M. I. Hossain, and Y. Okamura. 2011. Coupling of the phosphatase activity of Ci-VSP to its voltage sensor activity over the entire range of voltage sensitivity. *J. Physiol.* 589:2687–2705.
6. Kohout, S. C., M. H. Ulbrich, …, E. Y. Isacoff. 2008. Subunit organization and functional transitions in Ci-VSP. *Nat. Struct. Mol. Biol.* 15:106–108.
7. Kohout, S. C., S. C. Bell, …, E. Y. Isacoff. 2010. Electrochemical coupling in the voltage-dependent phosphatase Ci-VSP. *Nat. Chem. Biol.* 6:369–375.
8. Villalba-Galea, C. A., F. Miceli, …, F. Bezanilla. 2009. Coupling between the voltage-sensing and phosphatase domains of Ci-VSP. *J. Gen. Physiol.* 134:5–14.
9. Iwasaki, H., Y. Murata, …, Y. Okamura. 2008. A voltage-sensing phosphatase, Ci-VSP, which shares sequence identity with PTEN, dephosphorylates phosphatidylinositol 4,5-bisphosphate. *Proc. Natl. Acad. Sci. USA.* 105:7970–7975.
10. Murata, Y., and Y. Okamura. 2007. Depolarization activates the phosphoinositide phosphatase Ci-VSP, as detected in *Xenopus* oocytes coexpressing sensors of PIP2. *J. Physiol.* 583:875–889.
11. Okamura, Y., Y. Murata, and H. Iwasaki. 2009. Voltage-sensing phosphatase: actions and potentials. *J. Physiol.* 587:513–520.
12. Okamura, Y., and J. E. Dixon. 2011. Voltage-sensing phosphatase: its molecular relationship with PTEN. *Physiology (Bethesda).* 26:6–13.
13. Ledwell, J. L., and R. W. Aldrich. 1999. Mutations in the S4 region isolate the final voltage-dependent cooperative step in potassium channel activation. *J. Gen. Physiol.* 113:389–414.
14. Lu, Z., A. M. Klem, and Y. Ramu. 2001. Ion conduction pore is conserved among potassium channels. *Nature.* 413:809–813.
15. Alabi, A. A., M. I. Bahamonde, …, K. J. Swartz. 2007. Portability of paddle motif function and pharmacology in voltage sensors. *Nature.* 450:370–375.
16. Legros, C., V. Pollmann, …, O. Pongs. 2000. Generating a high affinity scorpion toxin receptor in KcsA-Kv1.3 chimeric potassium channels. *J. Biol. Chem.* 275:16918–16924.
17. Ottschytsch, N., A. L. Raes, …, D. J. Snyders. 2005. Domain analysis of Kv6.3, an electrically silent channel. *J. Physiol.* 568:737–747.
18. Lee, S. Y., A. Banerjee, and R. MacKinnon. 2009. Two separate interfaces between the voltage sensor and pore are required for the function of voltage-dependent K(+) channels. *PLoS Biol.* 7:e47.
19. Long, S. B., X. Tao, …, R. MacKinnon. 2007. Atomic structure of a voltage-dependent K+ channel in a lipid membrane-like environment. *Nature.* 450:376–382.
20. Lu, Z., A. M. Klem, and Y. Ramu. 2002. Coupling between voltage sensors and activation gate in voltage-gated K+ channels. *J. Gen. Physiol.* 120:663–676.
21. Smith-Maxwell, C. J., J. L. Ledwell, and R. W. Aldrich. 1998. Uncharged S4 residues and cooperativity in voltage-dependent potassium channel activation. *J. Gen. Physiol.* 111:421–439.
22. Smith-Maxwell, C. J., J. L. Ledwell, and R. W. Aldrich. 1998. Role of the S4 in cooperativity of voltage-dependent potassium channel activation. *J. Gen. Physiol.* 111:399–420.
23. Bosmans, F., M. F. Martin-Eauclaire, and K. J. Swartz. 2008. Deconstructing voltage sensor function and pharmacology in sodium channels. *Nature.* 456:202–208.
24. Coetzee, W. A., Y. Amarillo, …, B. Rudy. 1999. Molecular diversity of K+ channels. *Ann. N. Y. Acad. Sci.* 868:233–285.
25. Rudy, B., A. Chow, …, E. Vega-Saenz de Miera. 1999. Contributions of Kv3 channels to neuronal excitability. *Ann. N. Y. Acad. Sci.* 868:304–343.
26. Kanemasa, T., L. Gan, …, L. K. Kaczmarek. 1995. Electrophysiological and pharmacological characterization of a mammalian Shaw channel expressed in NIH 3T3 fibroblasts. *J. Neurophysiol.* 74: 207–217.
27. Lundby, A., H. Mutoh, …, T. Knöpfel. 2008. Engineering of a genetically encodable fluorescent voltage sensor exploiting fast Ci-VSP voltage-sensing movements. *PLoS ONE.* 3:e2514.
28. Dimitrov, D., Y. He, …, T. Knöpfel. 2007. Engineering and characterization of an enhanced fluorescent protein voltage sensor. *PLoS ONE.* 2:e440.
29. Lacroix, J. J., A. J. Labro, and F. Bezanilla. 2011. Properties of deactivation gating currents in *Shaker* channels. *Biophys. J.* 100:L28–L30.
30. Villalba-Galea, C. A., W. Sandtner, …, F. Bezanilla. 2008. S4-based voltage sensors have three major conformations. *Proc. Natl. Acad. Sci. USA.* 105:17600–17607.
31. Tao, X., A. Lee, …, R. MacKinnon. 2010. A gating charge transfer center in voltage sensors. *Science.* 328:67–73.
32. Lacroix, J. J., and F. Bezanilla. 2011. Control of a final gating charge transition by a hydrophobic residue in the S2 segment of a K+ channel voltage sensor. *Proc. Natl. Acad. Sci. USA.* 108:6444–6449.
33. Xu, Y., Y. Ramu, and Z. Lu. 2010. A *shaker* K+ channel with a miniature engineered voltage sensor. *Cell.* 142:580–589.
34. Hong, K. H., and C. Miller. 2000. The lipid-protein interface of a *Shaker* K(+) channel. *J. Gen. Physiol.* 115:51–58.
35. Bocksteins, E., N. Ottschytsch, …, D. J. Snyders. 2011. Functional interactions between residues in the S1, S4, and S5 domains of Kv2.1. *Eur. Biophys. J.* 40:783–793.
36. DeCaen, P. G., V. Yarov-Yarovoy, …, W. A. Catterall. 2011. Gating charge interactions with the S1 segment during activation of a Na+ channel voltage sensor. *Proc. Natl. Acad. Sci. USA.* 108:18825–18830.
37. Lu, J., J. M. Robinson, …, C. Deutsch. 2001. T1-T1 interactions occur in ER membranes while nascent Kv peptides are still attached to ribosomes. *Biochemistry.* 40:10934–10946.
38. Bocksteins, E., A. J. Labro, …, D. J. Snyders. 2009. Conserved negative charges in the N-terminal tetramerization domain mediate efficient assembly of Kv2.1 and Kv2.1/Kv6.4 channels. *J. Biol. Chem.* 284: 31625–31634.
39. Bezanilla, F. 2000. The voltage sensor in voltage-dependent ion channels. *Physiol. Rev.* 80:555–592.
40. Chahine, M., S. Pilote, …, C. Sato. 2004. Role of arginine residues on the S4 segment of the Bacillus halodurans Na+ channel in voltage-sensing. *J. Membr. Biol.* 201:9–24.
41. Miceli, F., M. V. Soldovieri, …, M. Taglialatela. 2008. Gating consequences of charge neutralization of arginine residues in the S4 segment of K(v)7.2, an epilepsy-linked K+ channel subunit. *Biophys. J.* 95: 2254–2264.
42. Glauner, K. S., L. M. Mannuzzu, …, E. Y. Isacoff. 1999. Spectroscopic mapping of voltage sensor movement in the *Shaker* potassium channel. *Nature.* 402:813–817.
43. Chanda, B., and F. Bezanilla. 2002. Tracking voltage-dependent conformational changes in skeletal muscle sodium channel during activation. *J. Gen. Physiol.* 120:629–645.
44. Klemic, K. G., G. E. Kirsch, and S. W. Jones. 2001. U-type inactivation of Kv3.1 and *Shaker* potassium channels. *Biophys. J.* 81:814–826.
45. Villalba-Galea, C. A., W. Sandtner, …, F. Bezanilla. 2009. Charge movement of a voltage-sensitive fluorescent protein. *Biophys. J.* 96: L19–L21.
46. Looger, L. L., and O. Griesbeck. 2012. Genetically encoded neural activity indicators. *Curr. Opin. Neurobiol.* 22:18–23.
47. Walton, R. D., R. M. Smith, …, A. M. Pertsov. 2012. Extracting surface activation time from the optically recorded action potential in three-dimensional myocardium. *Biophys. J.* 102:30–38.
48. Akemann, W., H. Mutoh, …, T. Knöpfel. 2010. Imaging brain electric signals with genetically targeted voltage-sensitive fluorescent proteins. *Nat. Methods.* 7:643–649.